

FAILURE INVESTIGATION OF STEAM BOILER TUBE IN PETROLEUM REFINERY

Gabriel ESSIEN¹, Jonathan UKPAI², Paul T. ELIJAH³

¹Facilities Maintenance, Nigerian Petroleum Development Company Limited (NNPC), Nigeria
Email: gabriel.essien@nnpcgroup.com

²Deputy Director, Engineering & Technology, Dept. of Polytechnic Programs, National Board for Technical Education (NBTE), Kaduna, Nigeria
Email: jonukupai@gmail.com

³Department of Mechanical Engineering, Nigeria Maritime University, Okerenkoko, Delta State, Nigeria
Email: paul.elijah@nmu.edu.ng

ABSTRACT

Failure investigation was carried out on steam boiler tubes through visual inspection, chemical analysis, and metallurgical analysis. Failure was in the form of thin/micro cracks along the length of the tubes which were located at the girth welding joint of tubes. Experimental results revealed that the cracking was from inward to outward of the tube thickness. Discontinuities/cavities were observed in the welded region which might have occurred due to lack of fusion of base metal and the weld metal. Cracks were initiated from the sharp corner/crack tip of the cavities/discontinuities present at the welded region under the action of hoop/ thermal stress existed during the operation. Nature of the crack propagation indicates the case of typical hydrogen induced cracking. Moreover, the presence of the cavities/ discontinuities reduced the cross-sectional area of tubes resulting increased stress intensity. Increased stress beyond the flow stress of the material assisted by hydrogen-induced effect resulted the cracking of the tubes. In order to mitigate the problem, proper welding of tubes joints should be carried out followed by proper inspection after weld. Secondly, hydrogen dissolution during welding should be prevented and treatment for its removal after welding should be carried out Failure of tubes in boiler may occur due to various reasons. These include failures due to creep, corrosion, erosion, overheating and a host of other reasons. This project deals with the probable cause(s) of failure and also suggests remedial action to prevent similar repetitive failure in future. Visual examination, dimensional measurement, chemical analysis, oxide scale thickness measurement and micro structural examination were carried to ascertain the probable cause(s) of failure of inner leg of platen super heater tube. The inner surface of the failed portion of the tube was covered with a white deposit. The elemental composition of inner surface containing adherent deposits reveals Al, Si, Mg, Fe etc. This is possibly due to the presence of aluminum silicate, magnesium silicate, and calcium silicate in inner surface of the tube, which results in poor conductivity. Insulating effect of this poor conductive deposit on the inner surface caused localized overheating of tube metal leading to accelerated creep damage and premature failure of the tube. Inferior quality of de-superheated spray water used to control the steam temperature was identified as the source of white deposit.

1.0 INTRODUCTION

Boiler tubes are usually manufactured using alloy materials which can withstand both high temperature from the flue gases and high pressure steam generation within the tube (Callister, 2003). The use for better boiler efficiency, they also allow reduction in volumes of material for fabrication, both which promotes positive economy benefits.

According to Viswanathan (1993), boiler tubes are often categorised into three groups of alloys; carbon steels, ferritic alloys and austenitic stainless alloys in which all the tubes are then graded according to its material compositions. The material grades listed by the author are based on the American Society of Mechanical Engineers (ASME) standards. There can be many reasons for boiler tube failures. It may occur due to extreme service conditions, poor maintenance or it may happen due to design fault or selection of wrong material. Identifying the failure mechanism is very important to prevent its recurrence (Spurr, 1959; Hutchings and Unterweiser, 1981; French, 1993; Imran, 2014; Elijah and Ezeife, 2020).

Relatively simple materials are designed and constructed to function effectively as boiler tubes under high temperature and high pressure conditions. The tubes are subject to potential degradation by a variety of mechanical and thermal stresses and potential environmental attack on both the fluid- and fire-/gas-side of the tube. If there are no breakdowns from the original design conditions, water touched tubes such as water wall and economizer tubes are designed for and should have essentially infinite life. The case for steam-touched tubes such as super heater (SH) and re-heater (RH) tubes is somewhat different. These tubes are affected by the inevitability of creep-limited lifetime, although lifetimes in excess of 200,000 operating hours are achievable. Unfortunately, boiler tube failures (BTFs) and cycle chemistry corrosion and deposition problems in fossil steam plants remain significant and pervasive, leading causes of availability and performance losses worldwide. This field guide provides a description of the mechanism producing the failure, identifies the contributing causes of the degradation, presents immediate actions that can be taken to remove or reduce the effect of the contributing causes, and addresses the potential ramifications or implications to other parts of the boiler unit (Benac and Swaminathan, 2002).

The function of the boiler is to convert water into superheated steam, which is then delivered to turbine to generate electricity (Bamrotwar & Deshpande, 2014). Pulverized coal is the common fuel used in boiler along with preheated air. The boiler consists of different critical components like economizer, water wall, super heater and reheater tubes. Thermal power plant boiler is one of the critical equipment for the power generation industries. In the present situation of power generation, pulverized coal fired power stations are the backbones of industrial development in the country, thus necessitating their maximum availability in terms of plant load factor (PLF).

At the same time reliability and safety aspect is also to be considered. The major percentage of the forced shutdown of the power stations is from boiler side. So it is necessary to predict the probable root cause/ causes of the forced outages and also the remedial action to prevent the recurrence of similar failure in future. A drum type utility Boiler for thermal power generation typically consists of different pressure parts tubes like water wall, economizer, super heater and reheater (Bhowmick, 2011). Different damage mechanism like creep, fatigue, erosion and corrosion are responsible of the different pressure parts tube failure.

The intent of this study is to present a clear explanation on the reasons why large number of repeat boiler tube failures (i.e same failure mechanism, same root-cause, same tube, etc.) occur in fossil-fired boilers. It describe the six requirements for a formalized boiler tube failure prevention program, discuss twenty-two common tube failure mechanisms in terms of typical locations, appearances, root causes, corrective action (Lee et al., 2009). Failure due to improper welding of the boiler tubes may also be one of the reasons for a power plant shutdown. Some of the characteristic modes of failure that occur because of an improper welding process of boiler tubes are weld cracking/ hydrogen cracking, slag inclusions, incomplete fusion, under fill/incomplete joints, porosity, distortion, etc. (Dhua, 2010; ASM Handbook, 2002; Cieslak, 1993).

2.0 MATERIALS AND METHOD

The purpose of the steam boiler is to generate operation utility steam for turbine, pumps and as heating medium in heat exchangers. A case study of a typical boiler tubes that have seen a service life of 22 years so far against its design life of 30 years. In view of the severe damage and leakage of the boiler tubes recorded overtime it became imperative to carry out root cause analysis of the equipment failure. The schematic sketch of the steam boiler as well as the operating parameter, fuel gas and feed water quality is shown in figure 1 and table 1 respectively.

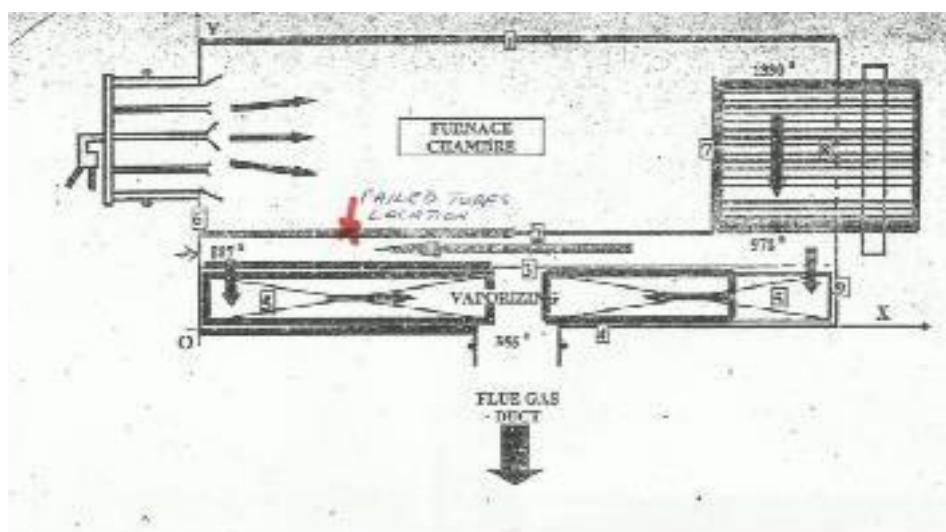


Figure 1: Schematic sketch of the steam boiler

Table 1: Schematic Sketch of the Steam Boiler

Boiler Fuel Gas and Water Chemistry detail:

| Boiler fuel sample analysed (11-05-2011) | Boiler feed water parameters |
|---|--|
| <ul style="list-style-type: none"> • Fuel used: Low Pour Fuel Oil (LPFO) • S.G.@ 60/60°F = 0.9197 • Flash point: 107 deg C • Total Sulphur: 0.270 % mass • Kinematic viscosity @ 82 °C = 7.62Cst • Pour point = +18deg C • Ash Content = 0.009Wt % • Carbon residue = 4.40Wt % • Water < 0.05Wt % | <ul style="list-style-type: none"> • pH = 8.32 • Specific Conductivity = 7 • Iron (mg/L Fe) = < 0.01 • Oxygen Scav' (ppb carbohydrazide) = 359 • Silica (mg/ L SiO₂) = 0.35 |

Operating parameters of boiler:

| Sr. No. | PARAMETERS | VALUES | |
|---------|------------|-----------------------|------------------------|
| 1 | BOILER | Operating pressure | 52Kg/cm ² g |
| | | Operating temperature | 405/410°C |
| | | Steaming rate | 70 T/hr (average) |
| 2 | TUBES | Material | SA 210 Gr. A1 |
| 3 | DIMENSIONS | Outer diameter | 63.5mm |
| | | Thickness | 4.5mm |

In order to commence the boiler failure investigation, the two halves of the boiler tubes identified as Sample: A (taken from the furnace internal wall on the side facing the furnace chamber) and sample: B (taken from the furnace internal wall on the side facing the flue gas) were collected for detailed root cause investigation. The Failure investigation was done with following approach: Collection of background data & history of failure with available photographic evidences, visual examination, low magnification examination, chemical analysis, SEM analysis, EDS analysis, macrostructure examination, microstructure examination, tensile test, hardness & micro-hardness tests. Based on the investigative findings the root cause of the problem has been identified. Suitable recommendations in form of remedial measures have been suggested to avoid its reoccurrence in future.

2.1 Experimental Procedure

The failure analysis was performed for the failed tube, especially the bursting section of the tube. For examining the inner wall surface morphology of the tube, samples were prepared from different regions of the failed tube. The metallography samples were prepared by using standard metallographic techniques and etched with 4% nital solution. The microstructure was analyzed by optical microscope and scanning electron microscope (SEM) equipped with an energy dispersive X-ray (EDX) analysis facility. In addition, the chemical composition of the failed tube was analyzed by 725ES Agilent spectrometer.

2.1.1 Investigation Steps

B1: Visual Examination

Visual examination was carried out on sample received for investigation as shown in figure 2, 3 &4.



Figure 2: Tube Sample-A obtained from Furnace side for Investigation

In figure 2, the close-up view at the puncture location on the tube OD surface. The puncture contours are elongated in transverse direction and they are uneven. Thinning appears to have taken place at the contours. Surrounding areas is having corrosion patches that have peeled off intermittently.



Figure 2: The

Figure 3: The ID Surface views Showing Thick Crusts of Corrosion Scale

In figure 3 the ID surface views shows thick crusts of corrosion scale. It seems to be porous and the metalwastage is observed having deep and coarse craters.

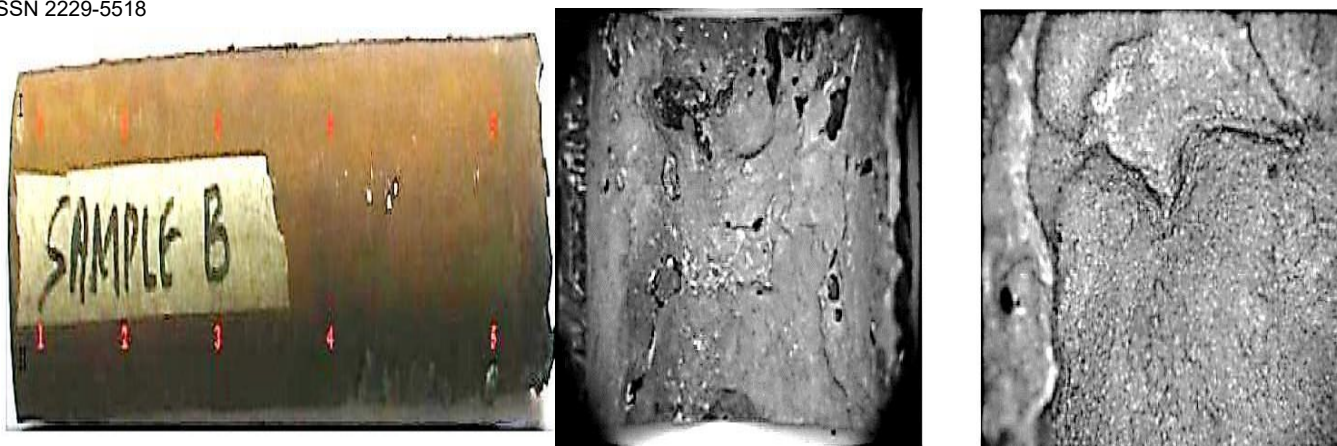


Figure 4: The ID Surface View of the Sample-B Showing Thin Layer of Corrosion Scale

In figure 4, it shows the tube sample-B obtained from tank bank side for investigation which is without any conspicuous puncture. The ID surface view of the sample-B show thin layer of corrosion scale which had peeled off at several places unlike Sample-A with thick layer of corrosion oxides.

RESULTS AND DISCUSSION

B2: Ultrasonic Thickness Measurements

The boiler tube material, ultrasonic machine and thickness measurement results for samples A and B are shown table 2a and b respectively.

Table 2a: Spots measurements

| Components | Boiler Tube |
|------------|----------------------|
| Machine | 37DL Plus Parametric |
| MOC | SA 210 Gr. A1 |

Table 2b: Results of Thickness Measurement

| Location | Sample-A | | Sample-B | |
|-------------------------------|----------|-----|----------|-----|
| | I | II | I | II |
| 1 | 3.5 | 4.1 | 5.6 | 5.9 |
| 2 | 4.2 | 4.0 | 5.5 | 5.6 |
| 3 | 4.1 | 3.5 | 5.6 | 5.2 |
| 4 | 3.8 | 3.6 | 5.6 | 5.8 |
| 5 | 4.0 | 3.9 | 5.8 | 5.9 |
| 3a Near Puncture | 3.4 | | - | - |
| 3b Near Puncture | 3.6 | | - | - |
| Minimum Thickness: 3.4 | | | | |

B3: Low Magnification Examination Analysis of Sample-A

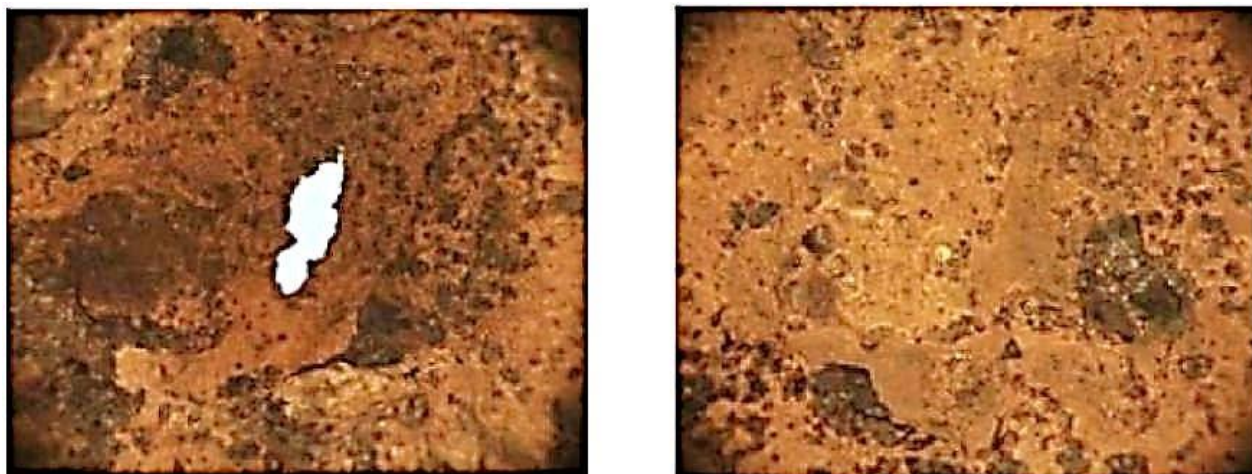


Figure 5: Tube Sample-A ID View in as Received Condition 4X

In figure 5, the low magnification view at puncture location at inner surface. Thinning is observed at puncture contours. Adjacent surrounding area is having fairly thick layer of scale which is porous. At a distances away from the puncture; thick layer of corrosion scale has peeled off at several places. Also the low magnification view on ID surface which is heavily corroded having fairly thick layer of porous corrosion scale which appears to be partly adherent.

B4: Chemical Analysis

Table 3: Result obtained through Optical Emission Spectroscopy for Sample-A

| <i>Elements</i> | <i>Measured</i> | <i>Required</i> |
|------------------------|-----------------|------------------|
| <i>Carbon (%)</i> | <i>0.150</i> | |
| <i>Sulphur (%)</i> | <i>0.010</i> | <i>0.035max.</i> |
| <i>Phosphorous (%)</i> | <i>0.022</i> | <i>0.035max.</i> |
| <i>Manganese (%)</i> | <i>0.680</i> | |
| <i>Silicon (%)</i> | <i>0.210</i> | |
| <i>Chromium (%)</i> | <i>0.100</i> | - |
| <i>Nickel (%)</i> | <i>0.098</i> | - |
| <i>Molybdenum (%)</i> | <i>0.025</i> | - |
| <i>Aluminum (%)</i> | <i>0.014</i> | - |
| <i>Copper (%)</i> | <i>0.200</i> | - |

Table 4: Result obtained through Optical Emission Spectroscopy for Sample-B

| <i>Elements</i> | <i>Measured</i> | <i>Required</i> |
|------------------------|-----------------|------------------|
| <i>Carbon (%)</i> | <i>0.160</i> | <i>0.27max.</i> |
| <i>Sulphur (%)</i> | <i>0.009</i> | <i>0.035max.</i> |
| <i>Phosphorous (%)</i> | <i>0.022</i> | <i>0.035max.</i> |
| <i>Manganese (%)</i> | <i>0.690</i> | <i>0.93max.</i> |
| <i>Silicon (%)</i> | <i>0.230</i> | <i>0.10min.</i> |
| <i>Chromium (%)</i> | <i>0.100</i> | - |
| <i>Nickel (%)</i> | <i>0.100</i> | - |
| <i>Molybdenum (%)</i> | <i>0.025</i> | - |
| <i>Aluminium (%)</i> | <i>0.010</i> | - |
| <i>Copper (%)</i> | <i>0.200</i> | - |

B6: Scanning Electron Microscopy

Scanning electron microscopy was conducted on ID surface to reveal more details about failure mechanism. The comments are given next to the individual photographs.

**Figure 6: Spot where SEM analysis was carried out.**

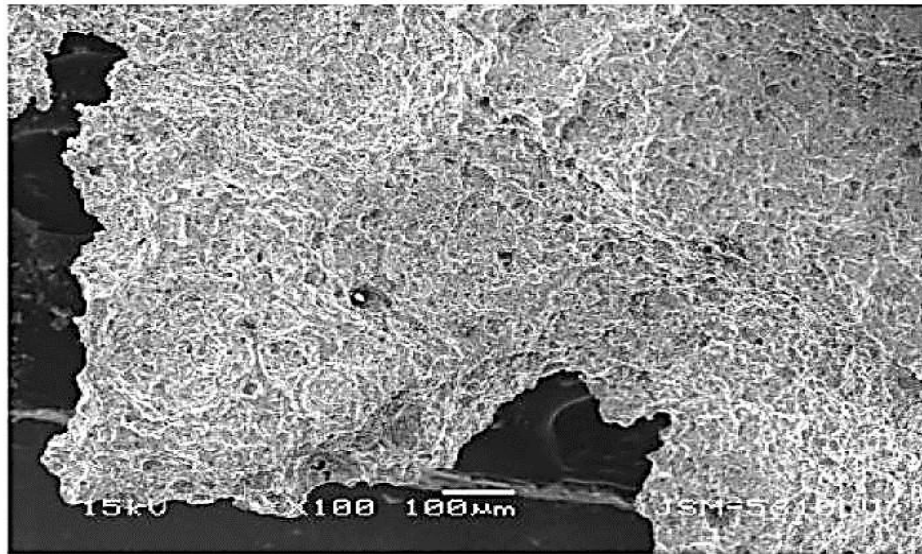


Figure 7: Tube Sample-A with low magnification view at the puncture contours which displays thinning by way of corrosion attack. Micro level corrosion attack is observed.

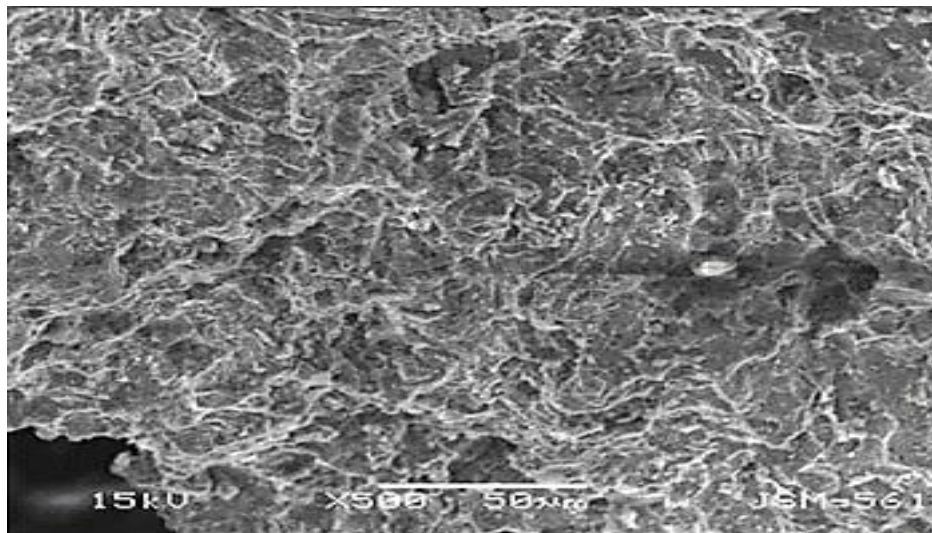


Figure 7: Tube Sample-A

Figure 8: Tube Sample-A with 500X magnification view at the puncture highlights corrosion attack leading to metal removal at micro level and pitting.

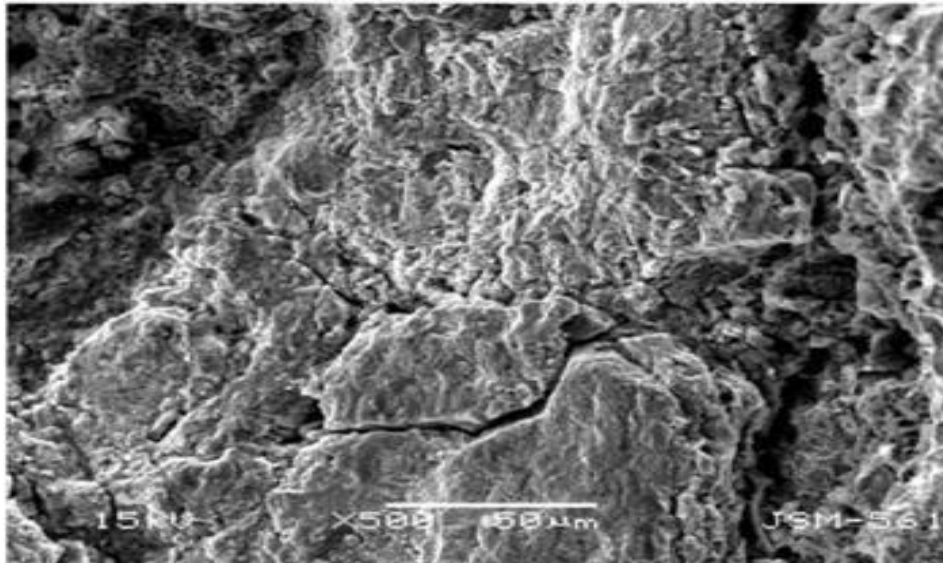


Figure 9: Tube Sample-A with 500X magnification view at the puncture also revealing incipient tendency for stress corrosion cracking.

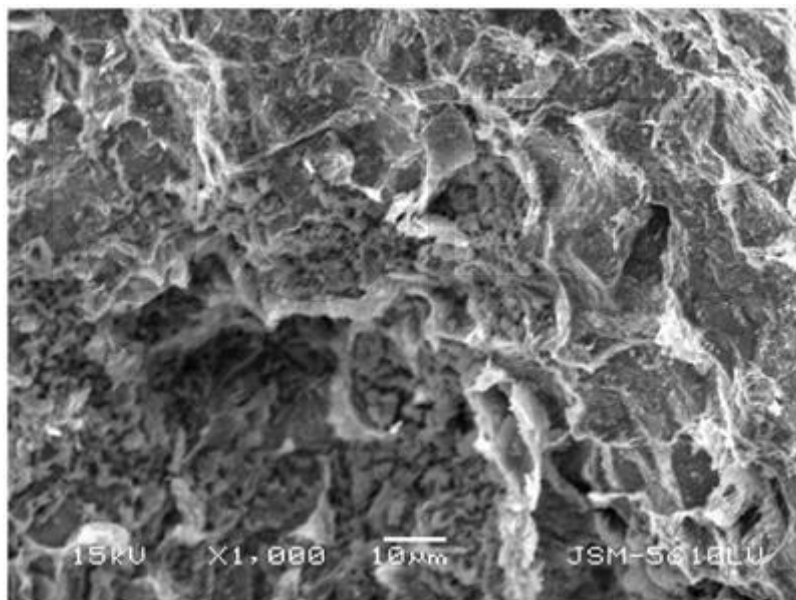


Figure 10: Tube Sample-A with 1000X magnification view near the puncture revealing micro pit filled with oxidescale formation on corroded surface.

B7: Energy Dispersive Spectroscopy (EDS) Analysis

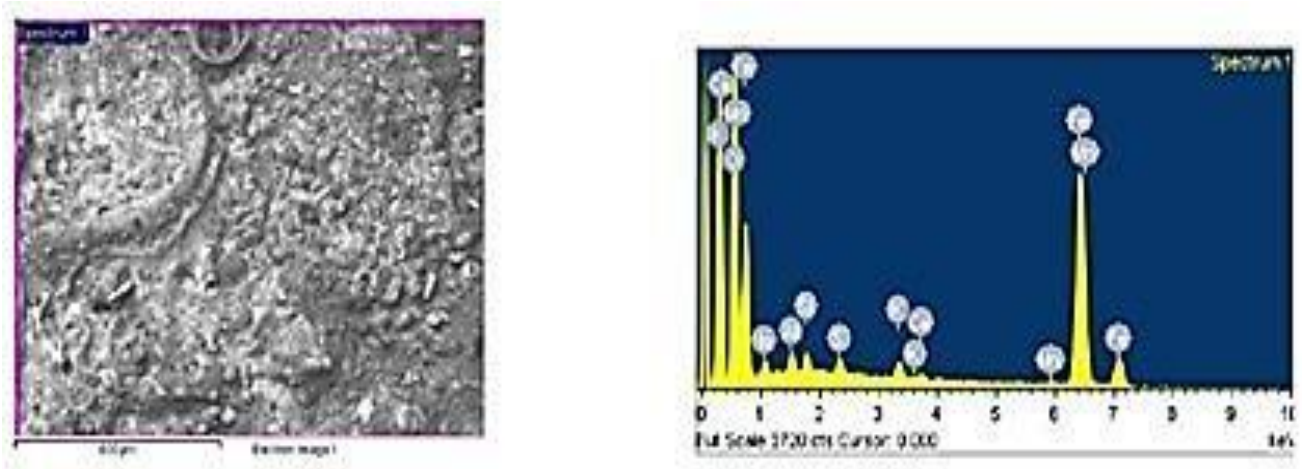


Figure 11: Result of EDS Analysis

Table 5: EDS analysis results on black scale at ID surface

| <i>Elements</i> | <i>% Composition</i> |
|------------------|----------------------|
| <i>Oxygen</i> | <i>27.68</i> |
| <i>Sodium</i> | <i>1.79</i> |
| <i>Aluminium</i> | <i>1.23</i> |
| <i>Silicon</i> | <i>1.19</i> |
| <i>Sulphur</i> | <i>0.99</i> |
| <i>Potassium</i> | <i>1.27</i> |
| <i>Calcium</i> | <i>0.45</i> |
| <i>Manganese</i> | <i>0.72</i> |
| <i>Iron</i> | <i>64.68</i> |

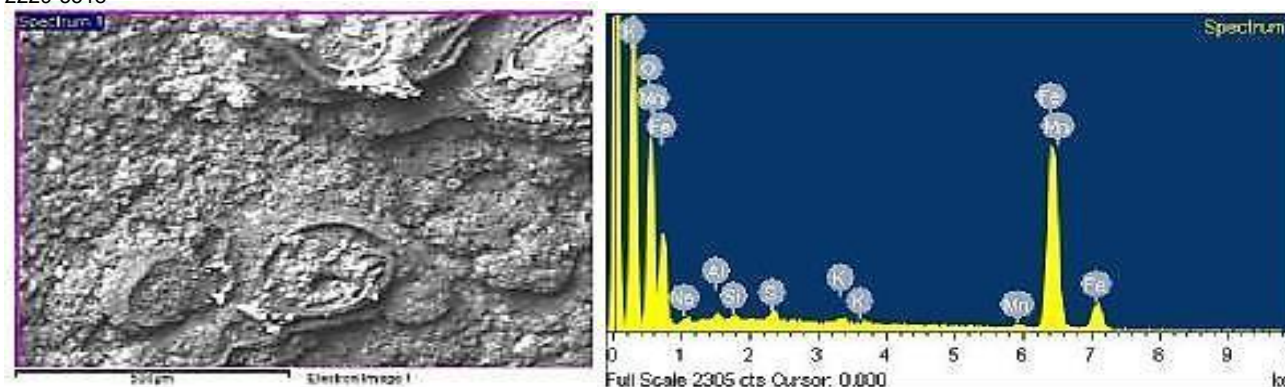


Figure 12: Result of EDS Analysis

Table 6: EDS analysis results on brown scale at ID surface

| <i>Elements</i> | <i>% Composition</i> |
|------------------|----------------------|
| <i>Oxygen</i> | <i>22.47</i> |
| <i>Sodium</i> | <i>0.79</i> |
| <i>Aluminium</i> | <i>0.63</i> |
| <i>Silicon</i> | <i>0.41</i> |
| <i>Sulphur</i> | <i>0.76</i> |
| <i>Potassium</i> | <i>0.46</i> |
| <i>Manganese</i> | <i>0.69</i> |
| <i>Iron</i> | <i>73.78</i> |

B8: Micro Structural Examination

Microstructure examination was carried out at various locations. Initially, the examination was done in “As polished” condition and then in “Etched” condition. **SAMPLE-A:** Away longitudinal cross-section, away transverse cross section and longitudinal cross section at puncture.

SAMPLE- B: Longitudinal cross section. Away longitudinal cross section-**Sample A**



Figure 13: Tube Sample-A specimen in a mounted condition with observed thinning of ID due to pitting like corrosion damage. The unetched view at ID showing corrosion damage with scaling indicating the gouging nature of corrosion damage.

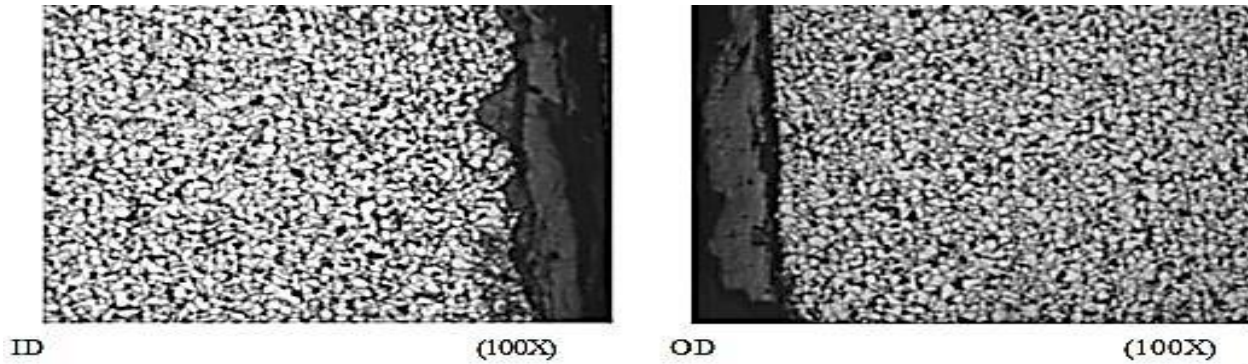


Figure 14: The etched view of ID surface showing pitting corrosion at the edge with matrix of fine ferrite and pearlite. The OD microstructure also showed fine ferrite and pearlite but no indication of pitting corrosion

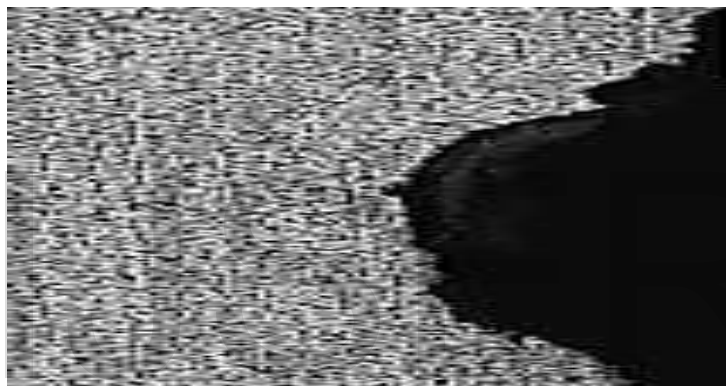


Figure 11:

Figure 15: The panoramic view at ID edge which highlights metal removal with gouging.

Away Transverse Cross Section – **Sample A**



Figure 16: The specimen viewed in a mounted condition showing ID damage by thinning. Also unetched view indicated signs of corrosion and scaling.

Away Transverse Cross Section –**Sample A**

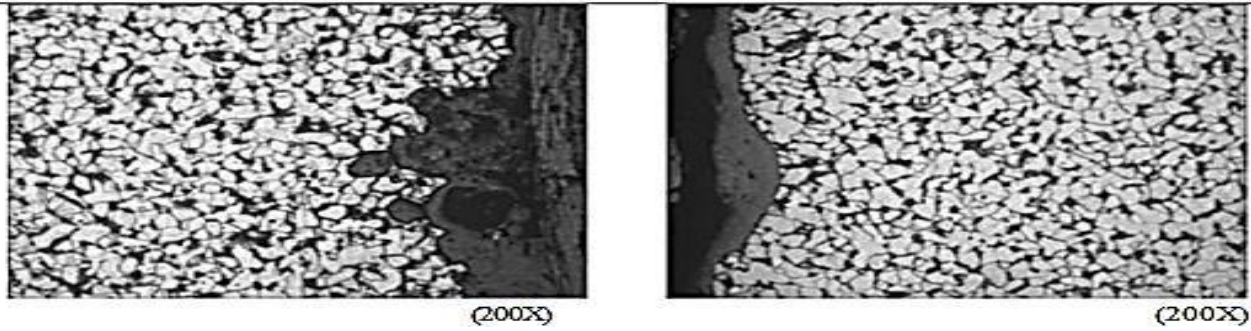


Figure 17: The etched views of OD & ID surfaces showing corrosion damage at the ID edges with signs of micropitting corrosion. The microstructure is fine grained ferrite and pearlite structure.

Puncture Transverse Cross Section –**Sample A**

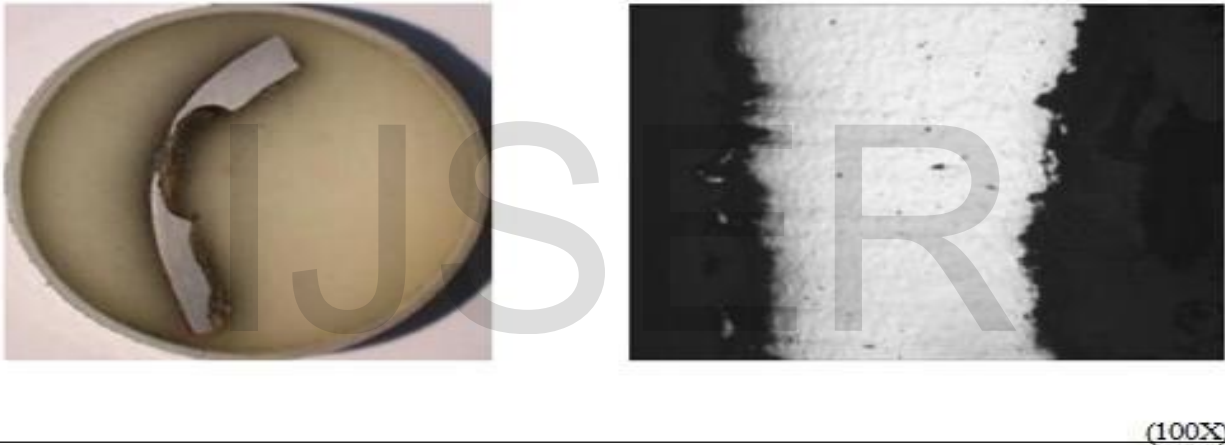


Figure 14:

Figure 18: The specimen viewed in as mounted condition showing coarse gouging from ID that eventually led to the puncture.

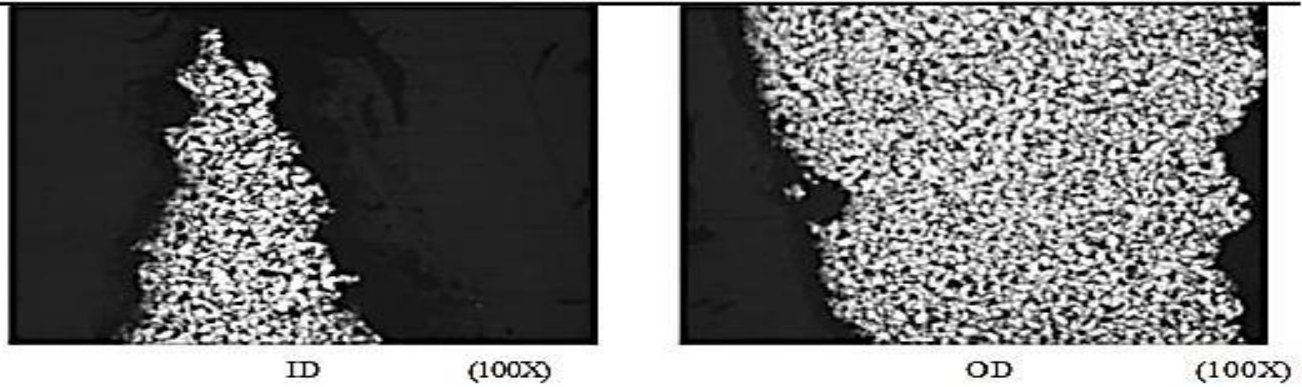


Figure 18: The etched views of OD & ID surfaces showing corrosion damage initiated from either side at the tip of puncture. The microstructure is fine grained ferrite and pearlite structure.

Longitudinal Cross-Section- Sample B



Figure 19: The specimen viewed in as mounted condition showing no significant corrosion damage at both the at ID and OD surfaces. The unetched view at ID showing marginal corrosion damage at the edge.

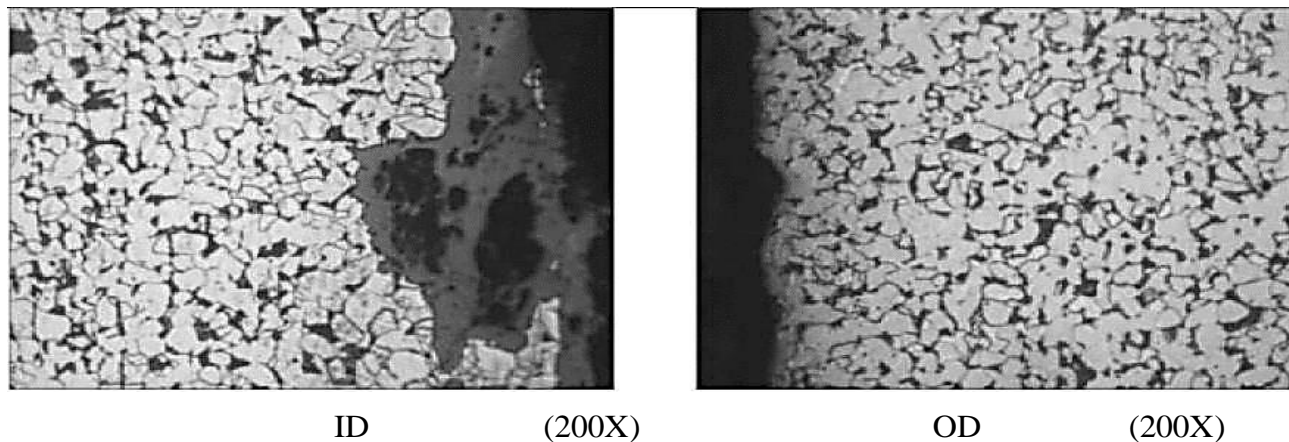


Figure 20: The ID microstructure of ferrite & pearlite with slight banding having marginal corrosion damage. The OD microstructure of ferrite and pearlite without significant any corrosion damage at the edges.

B9: TENSILE TEST

Tensile test was carried out on the test piece drawn from the Tube sample-B. The results are shown in table 7.

Table 7: Tensile Test Result

| <i>Physical Properties</i> | <i>Measured</i> | <i>Required Values (min)</i> |
|---|-----------------|------------------------------|
| <i>Thickness (mm)</i> | 4.75 | - |
| <i>Width (mm)</i> | 12.54 | - |
| <i>Area (mm²)</i> | 59.57 | - |
| <i>Gauge Length (mm)</i> | 50.60 | - |
| <i>Final Length (mm)</i> | 64.33 | - |
| <i>0.2% Proof Load (N)</i> | 21921 | - |
| <i>Ultimate Load (N)</i> | 30160 | - |
| <i>0.2% Proof Stress (N/mm²)</i> | 368 | 255 |
| <i>U. T. S. (N/mm²)</i> | 506 | 415 |
| <i>% Elongation</i> | 28.66 | 24 |
| <i>Fracture</i> | W.L.G. | - |

B10: HARDNESS MEASUREMENT

General hardness was measured on both the samples at different locations as shown in table 8.

Table 8: Bulk Hardness Values

| <i>Location</i> | <i>Hardness in “HRB” at 100 kg load</i> | | | | |
|--------------------------|---|----------|----------|----------------|-----------------|
| | <i>1</i> | <i>2</i> | <i>3</i> | <i>Average</i> | <i>Required</i> |
| <i>Sample-A: At core</i> | 78 | 78 | 79 | 78 | 79 Max. |
| <i>Sample-B: At core</i> | 78 | 78 | 77 | 78 | 79 Max. |

B11: Micro Hardness Measurement

Micro-hardness test was measured on Sample-A. The results are shown in table 9. The values at ID are significantly lower.

Table 9: Micro hardness Values

| <i>Location</i> | <i>Micro-Hardness in “VPN” at 100 gms. Load</i> |
|-----------------|---|
| <i>OD</i> | <i>199, 201</i> |
| <i>ID</i> | <i>148, 138</i> |
| <i>Core</i> | <i>163, 168</i> |
| <i>Near</i> | <i>208, 211</i> |

3.2 Discussion

- i. In the month of May 2011, leakage in form of severe perforation/punctures on 37 numbers of furnace internal wall tubes of boiler # 4 (70B04) having average steaming rate of 70T/hr was noticed. The failure occurred after 22 years of service against the design life of 30 years.
- ii. There were sporadic intermittent earlier failures which were repaired from time to time during breakdown maintenance shutdowns.
- iii. MOC of the tube is SA 210 Gr. A1 with diameter 63.5mm and thickness 4.5mm.
- iv. Visual examination indicates conspicuous puncture on sample –A which is from fire side. No puncture is seen on sample–B which is from water bank side. Severe thinning is noticed at the puncture contours and it is a little elongated in transverse direction.
- v. Visual examination further highlights thick crust of corrosion scale on ID surface of Sample-A. It is quite porous and has peeled off at several places.
- vi. Conversely, only a thin layer of corrosion scale is noticed on the ID surface of Sample-B.
- vii. Ultrasonic thickness measurements highlighted conspicuous uneven thinning at puncture location where as no such thinning is observed in Sample-B.
- viii. Low magnification view reveals thinning caused on ID surface of sample- A by corrosion attack and metal removal at puncture contours and appears like gouging. Both samples conform to SA 210 Gr. A1 with respect to chemical analysis.
- ix. Scanning Electron Microscopy (*SEM*) analysis reveals thinning due to severe corrosion attack at puncture contours by way of metal removal. Micro pitting with

- incipient tendency for cracking is also noticed at the place of thinning near puncture.
- x. EDS analysis on black scale on ID surface shows presence of oxygen, sodium, sulphur, potassium and chlorine. On brown scale at ID, oxygen, sodium, sulphur and potassium are present. EDS analysis on OD surface show presence of carbon, oxygen, sodium, sulphur, potassium and calcium.
 - xi. Optical microscopy highlighted Severe form of corrosion damage from ID (inner diameter) which is marginal at OD (outer diameter). It has typical appearance like metal gouging. Thick porous adherent scale is observed from ID side of the tube.
 - xii. General microstructure of both tubes showed fine grained ferrite and pearlite structure.
 - xiii. No indication of pitting corrosion of serious nature is noticed in Sample-B despite some corrosion damage at ID surface.
 - xiv. Tensile test results drawn from Sample-B are satisfactory in nature.
 - xv. Macro hardness values are acceptable on both the samples while micro hardness values are conspicuously lower on ID surface
 - xvi. The chemical composition of tube meets the standard requirements.
 - xvii. The ferrite-pearlite structure is found from the microstructure of the failed tube, which shows no obvious micro structural degradation, including no apparent pearlite spheroidization. However, a large number of corrosion pits exist on the inner wall surface of the fire-facing side. The absence of corrosion pits at the inner wall of the tube back side could be attributed the low operating temperature.
 - xviii. Oxidation corrosion of steels is easily accelerated due to the high affinity of oxygen to react with steel to form oxides. The kinetic of oxidation is higher at high temperatures than at room temperature.
 - xix. The inner wall surface of the fire-facing side is exposed to both the deaerated water and high temperature, and therefore undergoes oxidation corrosion. Correspondingly, reducing the oxidation contents in the deaerated water or reducing the maximum temperature would help minimize the fireside oxidation. However, the latter action has a direct impact on the efficiency and output of the boiler and usually never applied as a solution.

4.0 CONCLUSION

Corrosive condensate formed by the condensation of leaked out steam from superheater tubes, initiated SCC of wall tubes fixed in the water drum. During this course of this investigation, three major areas were encountered for which further work is needed. The first area is the creep behavior and life analysis of cracked boiler tubes. In our analysis we considered very simplified assumptions that the surface of the tube is clean and no crack initiated or pitting formed on the surface. The second major area of further study may be the cases of surface pitted and corroded boiler tubes. While operation, boiler tubes are exposed to abrasion and corrosion by the particles in the flue gas and steam and/or water respectively. The calculation of remaining life of boiler tubes on behalf of longitudinal thermal stress may give feasible result bit on behalf of efficiency calculation the result obtained through longitudinal stress. The calculation of efficiency on behalf of hoop stress value give more accurate result of efficiency on behalf of this paper the hoop stress values and formulas are to be used for calculation of efficiency for safe and reliable operation of modern thermal power plant. Poor thermal conductivity of the deposit found on the inner surface of the tube adversely affects the heat transfer and led to higher tube metal temperature causing premature failure of the tube. The undesirable steam quality and specific steam parameters at the platen super heater region facilitate precipitation of dissolved solutes in the steam on the inner surface of the tube. The presence of hard constituents like aluminium silicate, magnesium silicate etc. of water, used for attemperation in platen superheater region are responsible for the deposition at inner surface at high temperature.

ACKNOWLEDGEMENT

The researchers wish to acknowledge the top management staff of Nigerian National Petroleum Corporation (NNPC) particularly the group managing director, Mele Kolo Kyari, for creating an enabling environment that lead to the successful completion of this work.

REFERENCES

1. ASME, 2004. Section II Part D - Material Properties. ASME Boiler & Pressure Vessel Code. New York, NY: The American Society of Mechanical Engineers.
2. ASM International, 2002. Introduction to Steels and Cast Irons - Metallographer's Guide: Irons and Steels (#06040G). Ohio: ASM International.
3. A.S.M. Handbook, Failure Analysis and Prevention, vol. 11 (ASM International, Materials Park, 2002), pp. 319–399
4. Benac, D.J. and Swaminathan, V.P. (2002). ASM Handbook, AMS, USA 11, 289
5. Bamrotwar, S.R. & Deshpande, V.S. (2014). Root Cause Analysis and Economic Implication of Boiler Tube Failures in 210 MW Thermal Power Plant. *Journal of Mechanical and Civil Engineering*, 2014, 6-10.
6. Bhowmick, S. (2011). Ultrasonic Inspection for Wall Thickness Measurement at Thermal Power Stations. *International Journal of Engineering*, 4(1), 89-107.
7. Callister, W.D., (2003). Materials Science and Engineering: An Introduction. *Materials Science and Engineering: An Introduction*, 101.
8. Elijah, P. T. and Ezeife, N. C. (2020). Challenges of the Automobile Industry and Performance Analysis of an Assembly Plant in Nigeria, *Saudi Journal of Engineering and Technology*, 5(9), 337-342
9. French, D.N. (1993). Metallurgical Failures in Fossil Boilers, 2nd edition, Wiley, USA (1993).
10. Lee, N., Kim, S., Choe, B., Yoon, K. and Kwon, D. (2009). *Eng Fail Anal* 16 (2009), 2031.
11. Hutchings, F.R. and Unterweiser, P.M. (1981). Failure Analysis—The British Engine Technical Reports, American Society for Metals, USA (1981).
12. Cieslak, M.J. (1993). ASM Handbook, ASM International, Materials Park. 6s, 229-248
13. Spurr, J.C. *Corros Technol* 8(1959), 233
14. Dhua, S.K. (2010). *Engineering failure analysis*. 17, 1572-1579
15. Imran, M. (2014). *International Journal of advance Mechanical Engineering*, 4, 692

IJSER